The aqueous aragonite to calcite transformation: rate, mechanisms, and its role in the development of neomorphic fabrics

by

Kathleen M. McManus

Thesis submitted to the Faculty of
Virginia Polytechnic Institute and State University
in partial fulfillment of the requirements of the degree of
MASTER OF SCIENCE
in
Geology

APPROVED:

J. D. Rimstidt, Chairman

J. F. Read

R. K. Bambach

November, 1982

Blacksburg, Virginia

ACKNOWLEDGMENTS

The writer thanks Dr. J. D. Rimstidt for suggesting the project, providing technical guidance throughout its duration, and for helping to prepare the manuscript. Thanks also to Drs. J. F. Read and R. K. Bambach for their constructive criticism of the thesis.

Graditude is extended to David Banks for providing assistance in statistical analysis of the data, and to Ms. S. Chiang and Ms. O. Whaley who drafted the final figures.

To:
Mom and Dad for their
faith and love.
Also to Chris, Pat, John,
Anna, Dan, and Megan.

TABLE OF CONTENTS

LIST OF FIGURES

LIST OF TABLES

CHAPTER I

INTRODUCTION

In Recent marine environments the predominant carbonates are aragonite and high magnesium calcite, whereas those in ancient carbonate rocks are low magnesium calcite and dolomite. It is likely that the chemistry of marine waters has favored the precipitation of aragonite and high magnesium calcite throughout geologic time, so that the aragonite to calcite transformation has always been an important part of carbonate diagenesis. Despite the widespread occurence of this transformation, some metastable aragonite does persist in the rock record. Skeletal aragonite has been found preserved in ancient marine sediments as old as Lower Carboniferous (Hallam and O'Hara, 1962). Aragonite also occurs, outside its stability field at surface temperatures and pressures, in some blueschist facies metamorphic assembleges. Its anomalous persistence illustrates the importance of reaction kinetics over thermodynamic stability in controlling the transformation. The purpose of this study is to consider the mechanisms for the transformation of aragonite to calcite and how they might affect the rates of formation and the fabrics of the resulting calcite neospar (Davies, 1976).

The rate of the aragonite to calcite transformation has been measured by several workers under various conditions. The dry transformation proceeds very slowly at temperatures less than 375°C, even in terms of geologic time; whereas above 425°C it is extremely rapid (Carlson and Rosenfield, 1981; Rao, 1973; Kunzler and Goodell,

1970; Davies and Adams 1965; Brown et al., 1962; and Chaudron, 1954). On the other hand, the aqueous transformation proceeds rapidly, even at diagenetic temperatures of less than 100°C (this study; Bischoff, 1969; Bischoff and Fyfe, 1968; Metzger and Barnard, 1968; Taft, 1967; Fyfe and Bischoff, 1965; and Brown et al., 1962). This dramatic difference between the wet and dry reaction rates is a result of the transformation mechanisms. Solid-state, grain-boundary migration in the dry system is much slower and requires a higher activation energy than dissolution-precipitation in the aqueous system so that at diagenetic temperatures the solid state mechanism is not important. Diagenesis of sedimentary rocks takes place in the presence of an aqueous phase so that the persistence of metastable minerals in these environments must be due to factors affecting the rate of this wet reaction. These factors include temperature, solution chemisty, and size and shape of pores and crystallites. It is proposed here that the preservation of relict textures during neomorphism is strongly controlled by the geometry of the pores and the crystallites in the original aragonite.

A number of rate models have been used to explain these experimental results. A feasible rate equation for the dry system, based on Turnbull (1956), has been proposed by Carlson and Rosenfield (1981). Under aqueous conditions the transformation proceeds much more rapidly. Two types of models have been proposed to explain the observed rates for the aqueous reaction. The one presented by Fyfe and Bischoff (1968) is based on the combined effect

of nucleation and growth kinetics. They assume a constant rate of homogeneous nucleation and a growth rate independent of surface area. This model might be appropriate for their experiments in which no calcite was present at the onset of the experiment. However, in actual carbonate sediments there should be an abundance of calcite on which precipitation can take place (Schmalz, 1967; Matthews 1968, 1974). In these geologically more reasonable systems the rate limiting factor is likely to be the relative surface areas of the dissolving and precipitating phases. Rimstidt (in prep.) has derived a rate equation to describe this transformation for systems of discrete particles. As part of this study the rate of transformation of aragonite to calcite was measured in systems originally containing 5% calcite (to serve as growth sites and thus avoid a possible nucleation barrier). The data generated is used to test the validity of this rate model. The geometric factors in this model can be modified to explain the slower rates of microscale dissolution-precipitation observed in diagenesis. This supports the hypothesis that the preservation of relict textures during neomorphism is strongly controlled by the geometry of the pores and the crystallites in the original aragonite.

Calcite replacement fabrics can be catagorized according to the transformation mechanism as 1) passive dissolution-precipitation, 2) mesoscale dissolution-precipitation across a chalk zone, 3) microscale dissolution-precipitation across a fluid film, and 4) solid state grain boundary migration.

Passive dissolution is responsible for the formation of secondary

porosity, i.e. molds and/or vugs. It occurs when waters undersaturated with respect to calcium carbonate pass through carbonate sediments in vadose or phreatic environments. Precipitation of calcite in these molds or vugs may occur concurrently with dissolution (water undersaturated with respect to aragonite and saturated with respect to calcite) or sometime after dissolution (water undersaturated with respect to both aragonite and calcite followed by solutions saturated with respect to calcite). The fabric of this void filling calcite may be sparry (druse), with an increase in crystal size away from the substrate, or coarse equant, with a constant crystal size throughout. Criteria for distinguishing calcite spar from other forms of neomorphic calcite is outlined by Bathurst, (1975, p.417-419).

During mesoscale dissolution-precipitation a relatively porous reaction zone (chalk) is developed. This mechanism has been observed in scleractinian coral diagenesis (James, 1974; Pingitore, 1976) and produces a relatively coarse calcite neospar with moderate retention of precursor fabric detail. It is proposed that, by analogy to the above fabrics, coarse neomorphic calcite, after acicular marine cements, with moderate retention of precursor texture may be formed by a similar mechanism. These neomorphic calcites include neospar (Davies, 1976; Grover, 1981) and equant spar (Assereto and Folk, 1976).

The third mechanism, microscale dissolution-reprecipitation, is apparently responsible for the partial retention of precursor textures during neomorphism. This has been observed in both the alteration of

skeletal material, (Bathurst, 1958, 1964; Hudson, 1962, 1965; Banner and Wood, 1964; Dodd, 1966; Schroeder, 1973; and Sherer, 1977) and of marine cements (Cotter, 1966; Kendall and Tucker, 1973; Kendall, 1977; Mazzullo and Cys. 1977, 1979, Davies, 1977; Mazzullo, 1980; and Marshall, 1981). The neomorphic calcite after skeletal material generally contains organic inclusions which define the precursor fabric, irregular crystal boundaries, and exhibits undulose extinction. The process of transformation is often controlled by the original fabric (Pingitore, 1976; Schroeder, 1973; Banner and Wood, 1964). Microscale transformation of marine cements produces a variety of diagenetic calcite fabrics including radiaxial fibrous (Kendall and Tucker, 1973; Bathurst, 1975; Chafetz, 1979; and Marshall, 1981), radial fibrous (fascicular optic) (Kendall, 1977; Chafetz, 1979; and Marshall, 1981), divergent radial (Mazzullo and Cys, 1977, 1979; Mazzullo, 1980), and pseudoacicular (Grover, 1981). The differences in the fabrics are very likely dependant on the geometry of the original material (crystallite and pore sizes, boundary geometry, and internal porosity/permeability). This is because the rate of transformation at each site within the material is strongly controlled by the ratio of the surface areas of reactants and products to the amount of intergranular solution.

The last mechanism, solid state grain boundary migration, is restricted to retrogressive metamorphic textures in some blueschist facies metamorphic belts and is too slow to be of importance at diagenetic temperatures.

CHAPTER II

EXPERIMENTAL METHOD AND RESULTS

The rates measured in this study are for the overall reaction:

$$CaCO_3(\text{Aragonite}) \rightarrow Ca^{2+} + CO_3^{2-} \rightarrow CaCO_3(\text{Calcite})$$

This overall reaction includes the net rate of aragonite dissolution:

$$dn_A/dt = A_A(k_{+1} - k_{-1} Q^n) \quad (1)$$

and the net rate of calcite precipitation:

$$-dn_C/dt = A_C(k_{+2} - k_{-2} Q^n) \quad (2)$$

(Lasaga, 1981; and Sjoberg, 1976) where Q^n is the activity product of the aqueous species, A is the surface area of the solid phase, k_+ is the dissolution rate constant, k_- is the precipitation rate constant, and n=0.5. For systems with high CO_2 pressures, i.e. low pH, the rate equations are more complex (Plummer et al., 1979); however, under these conditions complete dissolution of the aragonite is likely rather than transformation to calcite. The overall rate measured in this study is a synthesis of rates of dissolution and precipitation of each of the solid phases.

The rate model was derived for a closed-system, aqueous, polymorphic transformation, where the transformation proceeds via a dissolution-precipitation mechanism and where nucleation is not the rate limiting step. The rate equation for this solid-aqueous-solid

reaction is dependent on the constantly changing, relative surface areas of the dissolving and precipitating phases. The derivation assumes a steady state such that the rate of aragonite dissolution (equation 1) equals the rate of calcite precipitation (equation 2). Under these conditions equation (1) can be set equal to equation (2). Solving for Q^n gives:

$$Q^n = (A_A k_{+1} + A_C k_{+2})/(A_A k_{-1} + A_C k_{-2}) \quad (3)$$

The surface area (A_i) of each of the solids, i, is related to the number of moles (n_i) of each by a geometric factor (b_i) and its molar volume (V_i):

$$A_i = b_i V_i^{2/3} n_i^{2/3} \quad (4)$$

The rate of formation of calcite can be found by substituting (4) into (3) to give Q^n in terms of the mole fraction of calcite present and then substituting (3) into (2). This form is simplified by letting:

$$C_1 = b_A V_A^{2/3} k_{-1} \quad (5)$$

and

$$C_2 = b_C V_C^{2/3} k_{-2} \quad (6)$$

It can be integrated to give:

$$t = [(3/C_2)(1-X^{2/3}) + (3/C_1)(X)^{2/3}]/[K_2-K_1] \quad (7)$$

Where X is the mole fraction calcite at time, t, and K_1 and K_2 are the thermodynamic equilibrium constants for aragonite and calcite solubilty, respectively.

In order to verify this equation, rates of aragonite to calcite transformation were measured at three temperatures. Experiments were run in 10 ml screw top Teflon bombs at 50±0.5°C, 77±1.0°C, and 101±1.0°C. In each bomb 0.2000±0.0005 grams of a 95% aragonite (needles, average size 13.5 µm long X 2.75 µm diameter) 5% calcite (rhombs, average size 5.3 µm on an edge) mixture were preheated to the run temperature. Six millimeters of preheated, distilled-deionized water (CO_2 free) were then added to each one and the bombs were incubated at run temperature for appropriate intervals. The percent calcite in the run products was determined by X-ray diffraction using a correlation chart constructed according to Davies and Hooper (1963) (Appendix 1). The pH, measured at 25°C at the end of each run, was approximately 7.5. Synthetic aragonite was prepared by mixing hot (80°C) 0.05m solutions of $NH_4(CO_3)_2$ and $CaCl_2$ following the proceedure of Katz (1973). Calcite, used to seed the material, was produced by transforming the synthetic aragonite in 6 ml of distilled-deionized water at 101±1.0°C. The 95% aragonite 5% calcite mixture

was chosen in order to minimize any effect of calcite nucleation (Appendix 1).

Graphs of mole fraction calcite versus time (Figs. 1, 2, 3), constructed using rate data from the aragonite to calcite experiments (Table 1), show that the general shape of each curve (Fig. 1, 2, and 3) is fit by equation 7 (solid lines). However, the curvature at the beginning of each experiment is more pronounced than is predicted by the equation. This may represent epitaxial calcite nucleation on the aragonite that is not accounted for by the rate model. In general there are three regimes for this reaction. Initially ($X \leq 0.2$) there is a gradual increase in the rate, which is limited by the surface area of the calcite grains, as the surface area of the calcite grows and approaches that of the aragonite (Fig. 4). When the surface area of calcite is nearly equal to that of aragonite, ($0.2 \leq X \leq 0.8$), the rate reaches a maximum. Finally, as most of the aragonite dissolves away, its surface area becomes rate limiting ($X \geq 0.8$) so there is a gradual decrease in the transformation rate to zero as the aragonite grains disappear. From equation (3) it is possible to calculate the ion activity product ($Q^n = aCa^{2+}aCO^{2-}$). Figure 5 shows that the solution is at first nearly in equilibrium with aragonite and as the reaction proceeds it decreases to equilibrium with calcite, when $X = 1$.

This rate model was derived for discrete, uniform particles of reactant and product but it should fit other situations provided b is suitably modified. In fact, Metzger and Barnard (1968) found the

Figure 1. Mole fraction calcite as a function of time for experiments run at 50°C.

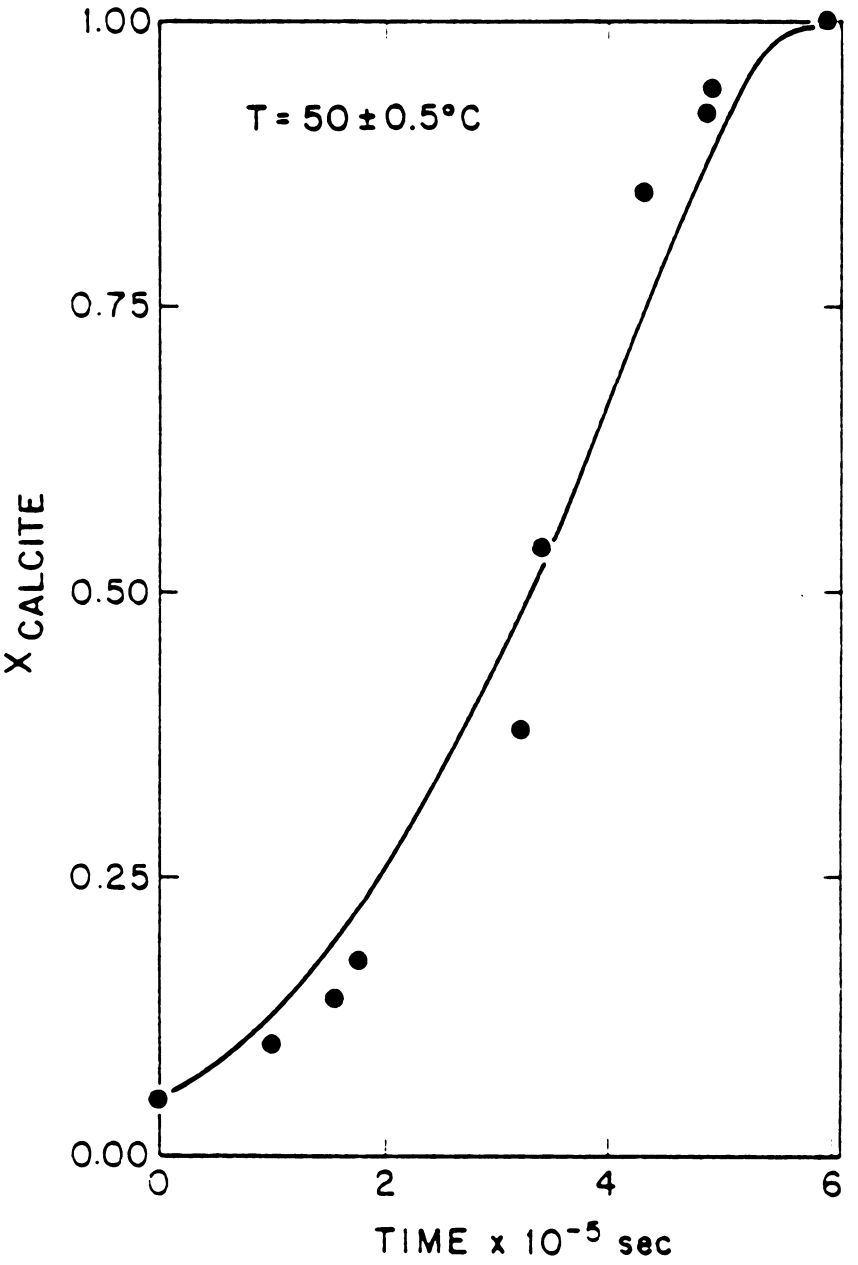
1.00
0.75
0.50
0.25
0.00
T = 50 ± 0.5°C
X CALCITE
0
2
4
6
TIME x 10⁻⁵ sec

Figure 2. Mole fraction calcite as a function of time for experiments run at 77°C.

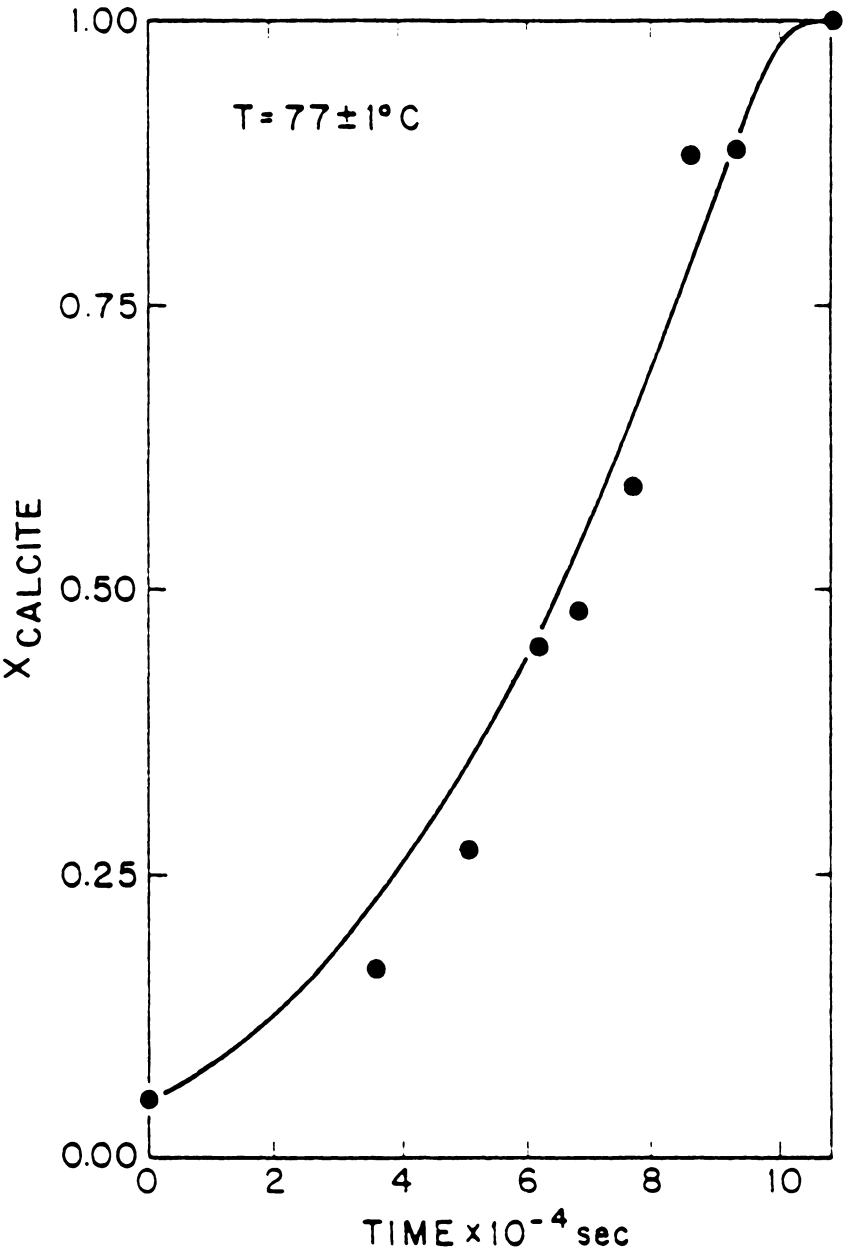
1.00
0.75
0.50
0.25
0.00
T = 77 ± 1°C
X CALCITE
0
2
4
6
8
10
TIME x 10⁻⁴ sec

Figure 3. Mole fraction calcite as a function of time for experiments run at 101°C.

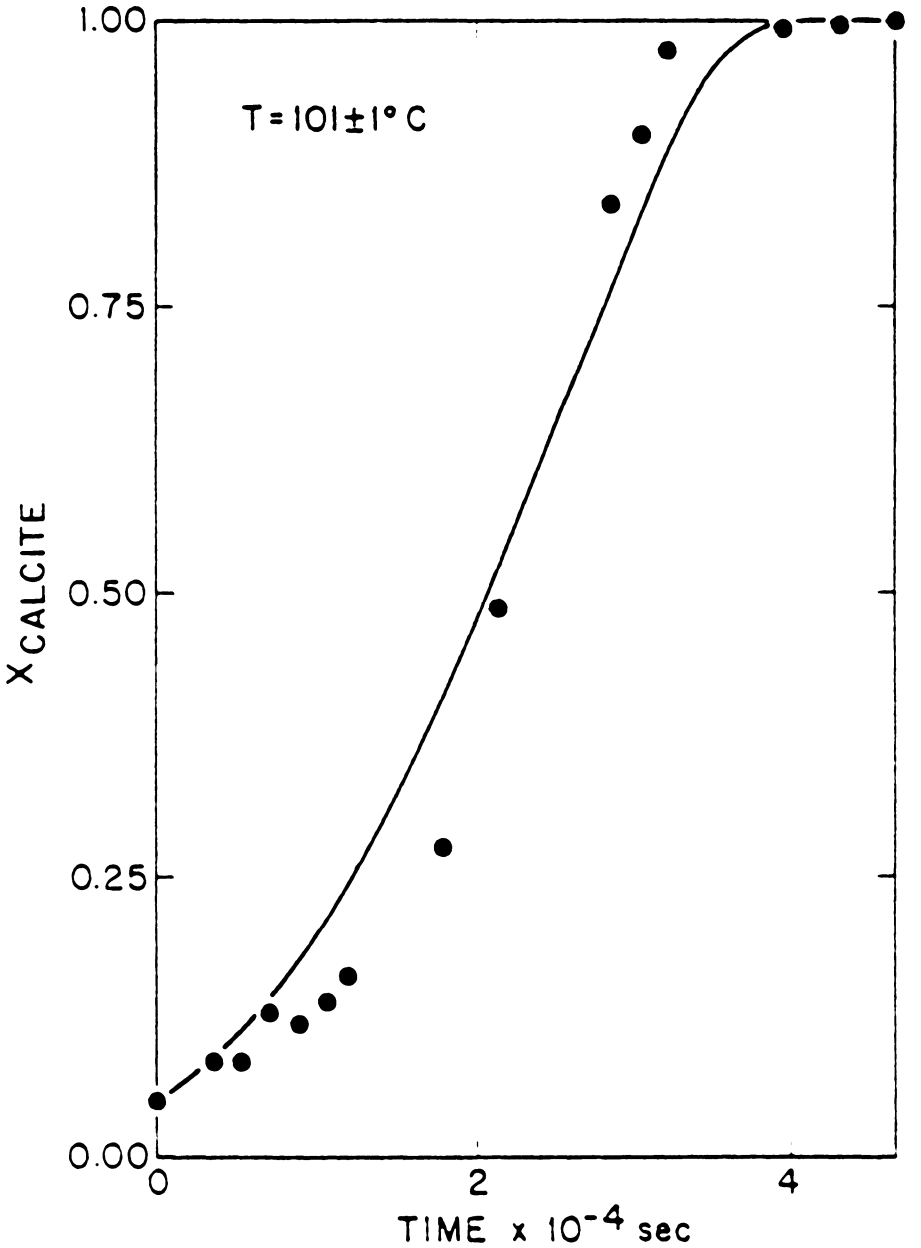
1.00
0.75
0.50
0.25
0.00
T = 101 ± 1° C
X CALCITE
0
2
4
TIME x 10⁻⁴ sec

TABLE 1. Mole fraction calcite versus time data from experiments.

Time, sec$X10^{-4}$	$\frac{I_{C1012}}{I_{A111}+I_{A012}+I_{C1012}} X100$	X
T=50±0.5°C		
0.00	11.4	0.05
9.84	24.2	0.10
15.33	32.0	0.14
18.27	37.6	0.17
23.09	42.0	0.22
32.13	61.0	0.38
34.20	75.0	0.54
43.36	94.5	0.85
48.96	97.2	0.92
49.68	98.8	0.94
59.76	100.0	1.00
T=77±1.0°C		
0.00	11.4	0.05
3.64	35.2	0.17
5.10	47.8	0.27
6.21	68.0	0.45
6.91	70.2	0.48
7.68	78.0	0.59
8.56	95.7	0.88
9.27	95.9	0.88
9.94	98.9	0.96
10.50	100.0	1.00
T=101±1.0°C		
0.00	11.4	0.05
0.36	21.6	0.08
0.54	21.3	0.08
0.72	29.2	0.13
0.90	27.2	0.12
1.08	32.4	0.14
1.20	33.8	0.16
1.80	49.8	0.27
2.16	69.6	0.48
2.88	94.6	0.84
3.06	97.7	0.90
3.24	99.0	0.98
3.96	99.6	0.99
4.32	99.9	0.99
4.68	100.0	1.00

Figure 4. Rate of calcite formation as a function of mole fraction calcite for the experiment at 50°C, as calculated from the rate model. Initially there is an increase in rate, which is limited by the surface area of calcite As the calcite surface area approaches that of aragonite, the rate reaches a maximum (slope = 0, when the surface area of calcite equals that of aragonite). This occurs before the 50% conversion point (at 0.25 mole fraction calcite) because there are many small calcite crystallites growing (large surface area per mole of solid) and a few large aragonite crystallites dissolving (small surface area per mole of solid). Finally, there is a decrease in rate as most of the aragonite dissolves away and its surface area becomes rate limiting.

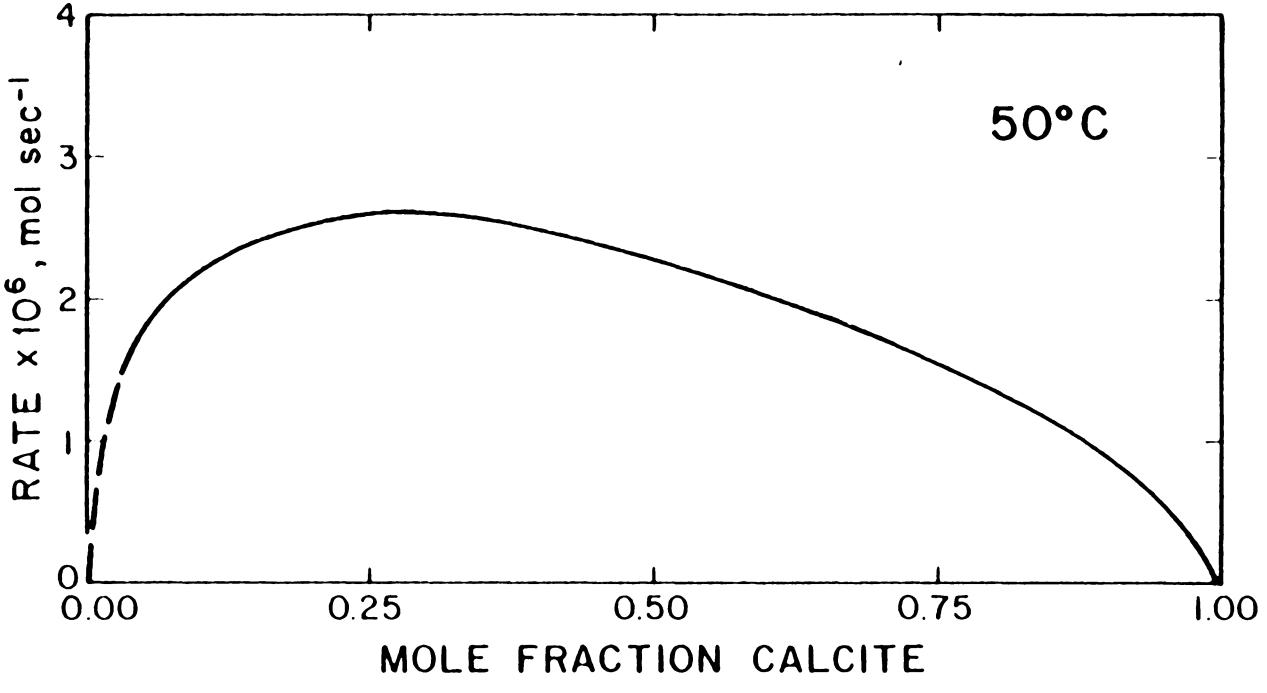
50°C
RATE x 10⁶, mol sec⁻¹
0
1
2
3
4
0.00
0.25
0.50
0.75
1.00
MOLE FRACTION CALCITE

Figure 5. Activity quotient ($Q^n = aCa^{2+} aCO^{2-}$) versus mole fraction calcite as calculated from the rate model.

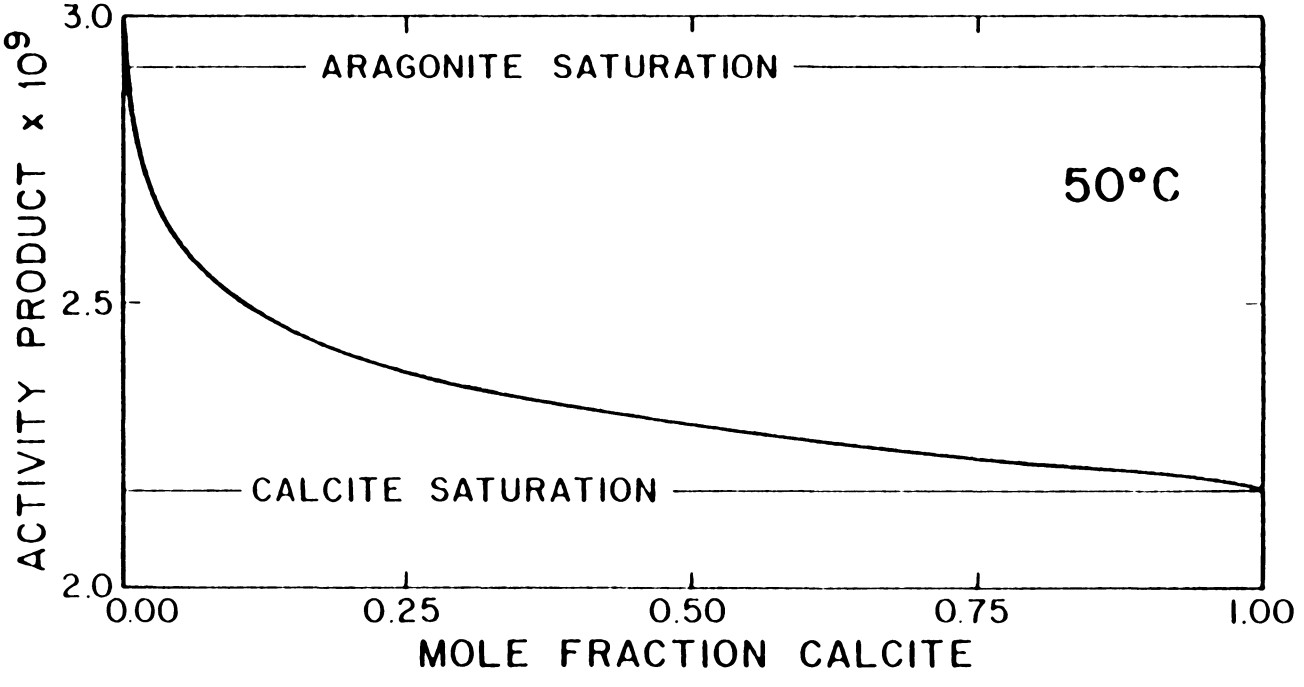
3.0
2.5
2.0
ACTIVITY PRODUCT x 10^9
ARAGONITE SATURATION
CALCITE SATURATION
50°C
0.00
0.25
0.50
0.75
1.00
MOLE FRACTION CALCITE

same general shape for the X versus t curve in their experiments using aragonite blocks. Thus, it appears that the relative surface areas of the reactant and product phases have a critical effect on the reaction rate in this more complex, geologically reasonable, experiment. The lower overall rates in the experiments by Metzger and Barnard reflects the smaller effective surface areas per mole of solid, as defined by b (equation 4), available to react with the solution in these tighter masses of crystallites. However, the fundamental mechanism appears to be the same (see also the discussion of apparent activation energies below).

A good way to compare the effect of temperature on the aragonite to calcite transformation rate is to plot the negative logarithm of the time to 50% conversion ($t_{\frac{1}{2}}$) versus $1000/T(K^{-1})$. In these experiments, it was found that the time to 50% conversion of aragonite to calcite at 101±1.0°C is approximately one twentieth that at 50±0.5°C. This increase in rate with increasing temperature can be expressed in terms of the Arrhenius equation:

$$\log (1/t_{\frac{1}{2}}) = \log A - (E_A' / 2.303R)1/T \qquad (8)$$

where $t_{\frac{1}{2}}$ is time to 50% conversion, A is a frequency factor, R is the gas constant ($J\ mol^{-1}\ K^{-1}$), E_A' is the apparent activation energy (see below), T is temperature in Kelvins. The increase in rate as a function of temperature has been well documented for both the wet

(this study; Bischoff, 1969; Metzger and Barnard, 1968; and Taft, 1967) and the dry (Carlson and Rosenfield, 1981; Rao, 1973; Davies and Adams, 1965; and Brown et al., 1962) systems. The overall rate measured in this and previous studies is the combination of a series of elementary reactions such that equation 8 gives only apparent activation energies (E_A'). Arrhenius plots of log ($1/t_{\frac{1}{2}}$) versus 1000/T were constructed using data from the studies listed above (Table 2, Fig. 6). Data from each series of experiments plot on a straight line, indicating constant apparent energy of activation and thus, a constant reaction mechanism over the temperature interval studied. The slope of each line equals $-E_A'/2.303R$ (Fig. 6) and was calculated using a least squares regression of the data in Table 2. The resulting values for apparent activation energy are listed in Table 3. The differences in slope, and therefore E_A', between the wet and the dry systems are a result of the different transformation mechanisms and readily demonstrate the catalytic effect of water, as the apparent activation energy for the wet transformation is much lower than that for the dry.

The activation energy is a useful clue for evaluating reaction mechanisms. It has been suggested that a very low E_A, less than 20 kJ mol^{-1}, represents reaction controlled by diffusion of aqueous species, and an E_A between 80 and 320 kJ mol^{-1} represent reactions in which strong covalent bonds are broken. Reaction with an

TABLE 2. Data for time to 50% calcite

TEMPERATURE, °C	log $t_{\frac{1}{2}}$, sec
Bischoff (1969) Aqueous	
62.0	5.4
75.0	5.2
90.0	5.0
108.0	4.9
120.0	4.7
Taft (1967) Aqueous	
23.0	6.8
70.0	5.1
Metzger and Barnard (1968) Aqueous	
200.0	6.0
250.0	5.4
300.0	4.8
this study Aqueous	
50.0	5.5
77.0	4.8
101.0	4.3
Brown et al. (1962) Dry	
400.0	5.3
420.0	4.5
440.0	3.4
460.0	2.9
Rao (1973) Dry	
420.0	4.2
430.0	3.6
440.0	3.5
Davies and Adams (1965) Dry	
400.0	3.5
450.0	1.7
500.0	1.4

Figure 6. Arrhenius plot of the logarithm of the time to 50% conversion of aragonite to calcite as a function of $1000/T$ (K^{-1}). Wet reaction-symbols: solid triangles, this study; solid circles, Taft, 1967; open circles, Bischoff, 1969; open squares, Metzger and Barnard, 1968. Dry reaction-symbols: solid squares, Brown et al., 1962; open triangls, Rao, 1973; solid circles, Davies and Adams, 1965.

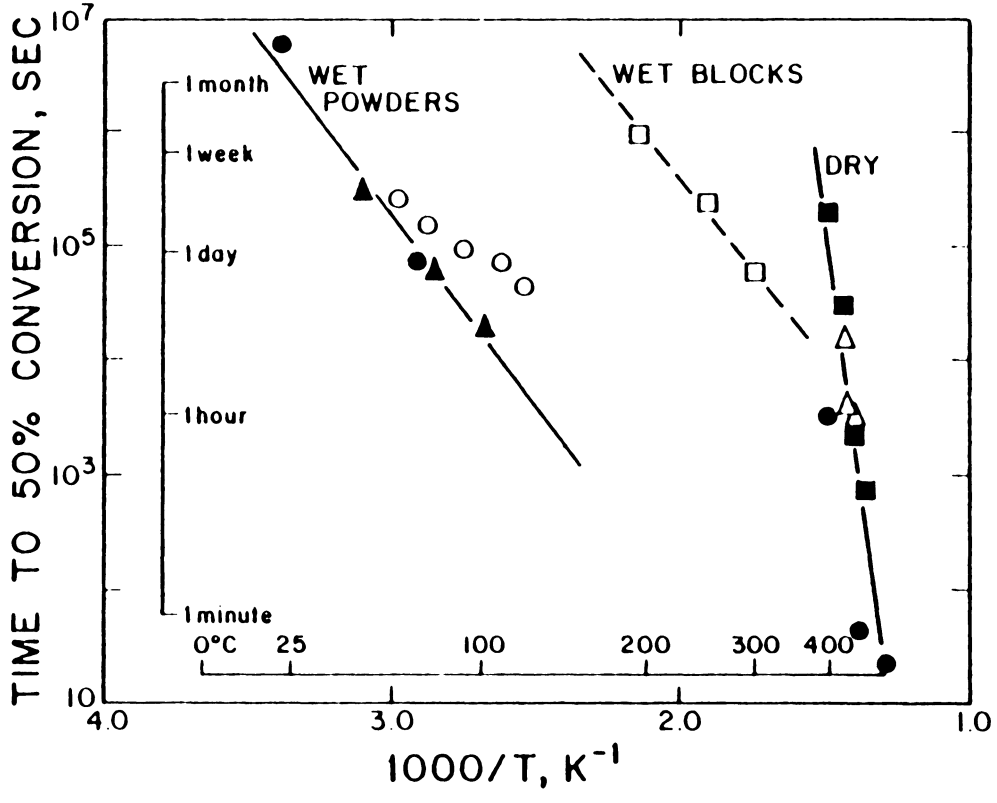
TIME TO 50% CONVERSION, SEC
10^7
10^5
10^3
10
1 month
1 week
1 day
1 hour
1 minute
WET POWDERS
WET BLOCKS
DRY
0°C
25
100
200
300
400
4.0
3.0
2.0
1.0
1000/T, K^{-1}

TABLE 3. Apparent activation energies calculated from the $t_{\frac{1}{2}}$ data.

Author	No. points	E_A kJ mol^{-1}
DRY TRANSFORMATION		
Brown et al. (1962)	4	372.9
Rao (1973)	3	395.3
Davies & Adams (1965)	3	218.9
SOLID AQUEOUS SOLID (LOW CO_2 PRESSURE)		
Metzger and Barnard (1968)	3	58.5
Taft (1967)	2	67.9
this study	3	55.2
ACID CATALYZED (HIGH CO_2 PRESSURE)		
Bischoff (1969)	5	27.6

intermediate E_A, 20 kJ mol^{-1} to 80 kJ mol^{-1}, are thought to be controlled by dissociation of ionic bonds, especially at surface defects (Lasaga, 1981). Under near equilibrium conditions, for the calcium carbonate-aqueous solution system, apparent E_A' calculated for $CaCO_3$ dissolution and/or precipitation (Berner and Morse, 1974; Sjoberg, 1976; and this study) fall within this intermediate range, thus indicating a surface defect controlled reaction, where the adsorption of H^+ ions to, and desorption of Ca^{2+} and CO_3^{2-} ions from the surface appears to be rate controlling (Berner and Morse, 1974). A surface controlled reaction is also supported by the dependence of the rate on the relative surface areas of the reactant and product phases, as verified in this study. Note that the results of Metzger and Barnard (1968) (solid blocks) plot on a line that parallels (similar E_A') those of this study and Taft (1967) (powders)(Fig. 6). This indicates that the fundamental reaction mechanism is the same in both cases but the rates were slower for the blocks because of the lower relative surface areas. The comparitively low E_A' from Bischoff (1969) suggests that their reaction might have been controlled by diffusion. This may be due to the use of more acidic solutions (higher CO_2 pressures) which leads to higher surface reaction rates (Berner and Morse, 1974). The much slower dry transformation has large values of E_A' reflecting the large amount of energy required for the solid state structural transformation in the absence of a catalyst (water).

The aqueous aragonite to calcite transformation proceeds via a dissolution-precipitation mechanism and occurs early in carbonate diagenesis (Steinen, 1982). Previous studies have shown that the rate of this reaction is influenced by temperature and by the solution composition; principally the inhibitors magnesium, phosphate, and sulfate (Taft, 1967; Fyfe and Bischoff, 1965; Metzger and Barnard, 1968; Bischoff and Fyfe, 1968; and Bischoff, 1969). In addition, however, this study shows that because the fundamental dissolution and precipitation rates are directly proportional to the surface areas of the solids, the overall rate of transformation is strongly influenced by grain geometry. That is grain size, shape and packing density. Thus, any petrologic studies of this transformation are likely to find that the nature of the product calcite is strongly influenced by the texture of the original aragonite.

CHAPTER III

GEOLOGIC APPLICATION

The rate and mechanism of the transformation of aragonite to calcite are dependent upon the geometry of the reacting system, the solution composition and the temperature. Based on the experimental findings presented here it is not surprising that most studies of neomorphic calcites find that the calcite textures are related to the original aragonite textures (this study; Land, 1970; Steinen and Matthews, 1973; Matthews, 1974; Friedman, 1975; Pingitore, 1976, 1982; Brand and Veizer, 1980; and Longman, 1980). This is because the aragonite to calcite transformation reaction is controlled by the b term in equation 4, which relates the amount of surface area available for reaction to the number of moles of material present. In sediments, this geometric factor reflects the distribution of solution in the sediment pores, and is controlled by the relative size and shape of the grains and the pores. The transformation rate is also dependent on the chemistry of the solution, especially the presence of inhibitors (Taft, 1967; Bischoff and Fyfe, 1968; Winland, 1969; Suess, 1969; Folk, 1974; Berner, 1975; and Walter and Hanor, 1979). The magnesium ion strongly inhibits the transformation at concentrations found in normal seawater ($Mg^{2+}:Ca^{2+}$=3.25:1, Berner, 1975), but has little effect at concentrations five percent less than that of normal seawater ($Mg^{2+}:Ca^{2+}$=3.1:1, Berner, 1975), or when $Mg^{2+}:Ca^{2+}$ is less than 2:1 (Folk, 1974). Reduction of the magnesium content in pore

fluids may occur by the influx of fresh water in the vadose-phreatic environments during subaereal exposure. It may also occur by dolomitization, or by clay diagenesis in the shallow burial environment (Folk, 1974). Thus, the principle diagenetic environments (as defined by solution chemistry and distribution of pore fluids, Longman, 1980) for the aragonite to calcite transformation are:

1) the meteoric vadose environment, where pores are intermittantly wet or dry,
2) the phreatic environment, where pores are filled with water ranging in composition from fresh to slightly saline (mixing zone), and
3) the shallow burial environment, where pores are continuously filled with connate waters, possibly saline brines depleted in Mg^{2+}.

Because they are subaqueous, the shallow burial and phreatic environments often have similar fluid/solid geometries. Thus, while the reaction rates may be different because of inhibitors, the overall geometry of the transformations are similar and similar neospar textures are produced. Finally, as was discussed previously, the transformation rate increases with temperature. However, because this transformation normally takes place during early diagensis temperature has little influence on neospar textures. However, the calcite textures produced by the aragonite to calcite transformation during early diagenesis may be subsequently altered by recrystallization during burial diagenesis. Thus, of the three variables that affect the

aragonite to calcite transformation (geometry, solution chemistry, and temperature), the geometry of the reacting system seems to have the most influence on the final calcite textures.

Three general transformation mechanisms have been proposed to explain the variability in diagenetic calcite textures and trace element chemistries. These processes are:

1) passive dissolution-precipitation (cm scale),

2) transformation across a chalk zone (mm scale), and

3) transformation across a thin fluid film (μm scale),

(Bathurst, 1958, 1964, 1975; Kinsman, 1969; Wardlaw et al., 1978; James, 1974; Pingitore, 1976, 1982; and Brand and Veizer, 1980). These mechanisms are grossly differentiated by the scale of the fluid/solid geometry. This classification is gradational and these mechanisms and their resulting textures may merge into one another depending on the availability of water to the system, the degree of calcium carbonate saturation, and the geometry (compactness, surface area, porsity/permeability) of the original material. More than one process therefore may be operative in a given diagenetic macroenvironment.

The diagenetic texture of a particular particle will be most dependent on the factors affecting the diagenetic microenvironment. Pingitore (1976) proposed that diagenesis is best described in terms of a mobile and immobile water system. In this system, alteration occurs by microscale dissolution-precipitation through immobile water held in a micropore reaction zone. These diagenetic sites are either physically

open or closed systems depending on the degree of isolation from the mobile water of the bulk aquifer. The bulk aquifer is the larger body of water which passes through the interparticle space within the sediment (Pingitore, 1976, 1982; Brand and Veizer, 1980)(Fig. 7). The degree of textural detail and isotope and trace element chemistry preserved after the transformation are then dependent on the scale (micron to millimeter) of the reaction zone and the degree of communication between, and chemistry of, the reaction zone and bulk aquifer waters (Pingitore, 1976, 1982; Lohmann, 1978; Brand and Veizer, 1980; and Sandberg, 1981). Based on the classification presented above it is clear that this two water system becomes less discrete as the scale of the intergranular spaces increases from microns to centimeters, so there is no distinction in the case of passive dissolution.

Passive dissolution-precipitation is the most rapid of the three transformation mechanisms. The large effective surface area per mole of solid available to react with solution produces a physically open system in which the reaction zone and aquifer are not differentiated. In this environment, the geometric term, b, would be quite large (about the same as in the powder transformation experiments) so the aragonite-calcite transformation rate would be fast. Transformation by this mechanism occurs when waters undersaturated with respect to aragonite pass through the sediment in either the vadose or phreatic environments. This results in the development of secondary porosity and the loss of all original texture of aragonite grains. Selective

Figure 7. Schematic illustration of the three principle pore geometries and the interaction of pore water with the bulk aquifer water. A) In microscale dissolution-precipitation the secondary pores contain a thin fluid film with very little, or no, communication between the reaction zone waters and those of the bulk aquifer. B) In mesoscale dissolution-precipitation the chalk zone pores have moderate communication between the reaction zone waters and those of the bulk aquifer. C) In macroscale dissolution-precipitation the reaction produces a void, so that the reaction zone waters are in complete communication with those of the bulk aquifer.

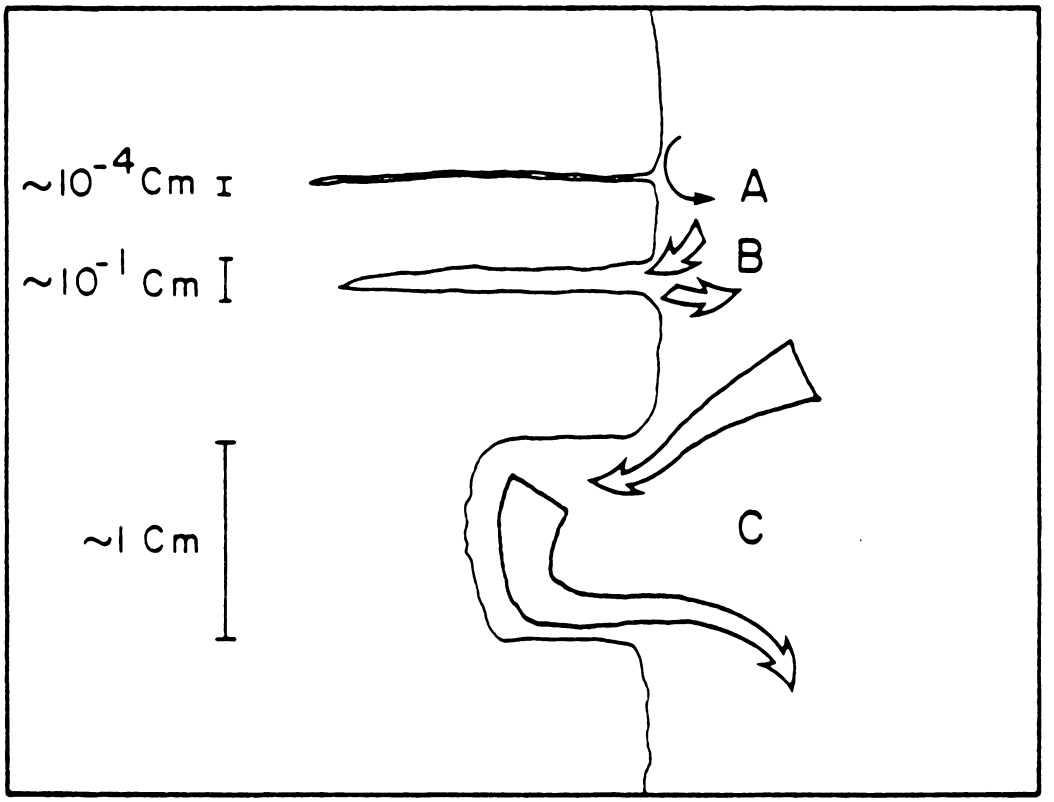
~10⁻⁴ Cm
~10⁻¹ Cm
~1 Cm
A
B
C

dissolution of aragonite occurs when waters are undersaturated with respect to aragonite and saturated with respect to calcite. The gross morphology of the precursor material may then be preserved, in the form of molds, casts or the outlines of micrite envelopes, when calcite is subsequently precipitated (Table 4, Fig. 8) (Bathurst, 1964; Dodd, 1966; Friedman, 1975). This is a common means of preservation of skeletal material but has not been recognized in the preservation of marine cements. The resulting calcite fabric is similar to that of primary calcite cements (Bathurst, 1964, 1975 p.417-419; Kendall, 1971) and may vary depending on the environment of precipitation. In the vadose environment calcite cement tends to have a pendant or meniscus habit (Dunham, 1971; Muller, 1971; Friedman, 1979; Grover, 1981) and to be relatively fine grained (Land, 1970; Pingitore, 1976). Spar precipitated in the phreatic environment is generally isopachous. It may have a porphyrotopic texture (Friedman, 1975)(Fig. 8B), or the grain size may be constant throughout (Folk, 1974) (Fig. 8A), and it is generally coarse grained (Land, 1970; Folk, 1973; Pingitore, 1976). The difference in vadose and phreatic spar is due to the difference in the availability of water to the system (Steinen and Matthews, 1973; Matthews, 1974; Friedman, 1975).

During mesoscale transformation through a chalk zone (no void developed) the ratio of surface area of reactant and product phases to the amount of solution is less than that of passive dissolution-precipitation and the rate of transformation is lower. A chalk zone is developed when waters, initially saturated to slightly undersaturated

TABLE 4. Aragonite transformation senarios and the resulting neospar textures.

PROCESS	ENVIRONMENT	STARTING MATERIAL		
		FOSSILS	OPEN ARAGONITE ACICULAR CEMENT	TIGHT ARAGONITE ACICULAR CEMENT
MACROSCALE DISSOLUTION PRECIPITATION (VOID)	VADOSE PHREATIC	VOID FILLING MOLD, CAST, MICRITE ENVELOPE	NOT RECOGNIZED	NOT RECOGNIZED
MESOSCALE DISSOLUTION PRECIPITATION (CHALK ZONE)	PHREATIC	COARSE BLOCKY CALCITE MODERATE PRESERVATION NOT CONFINED WITHIN THE ORIGINAL SHELL MATERIAL	COARSE BLOCKY CALCITE MODERATE PRESERVATION NEOSPAR (DAVIES, 1976) FINE EQUANT (ASSERETO AND FOLK, 1976)	COARSE BLOCKY CALCITE MODERATE PRESERVATION NEOSPAR (DAVIES, 1976)
MICROSCALE DISSOLUTION PRECIPITATION (THIN FLUID FILM)	PHREATIC VADOSE	FINE ANHEDRAL CALCITE GOOD PRESERVATION NOT CONFINED WITHIN THE ORIGINAL SHELL MATERIAL	FINE POLYCRYSTALLINE CALCITE GOOD PRESERVATION DIVERGENT RADIAL (MAZZULLO, 1980) PSEUDOACICULAR (GROVER, 1981)	COARSE CALCITE GOOD PRESERVATION RADIAXIAL FIBROUS (KENDALL AND TUCKER, 1973) RADIAL FIBROUS (FASCICULAR OPTIC, KENDALL, 1977)

Figure 8. Macroscale dissolution-precipitation textures (passive dissolution-precipitation). A) Passive dissolution of aragonitic corals with simultaneous precipitation of calcite, produces a coarse equant mosaic while (B) subsequent precipitation produces isopachous sparry (druse) calcite. Sketches adapted from James, 1974. Passive dissolution of aragonite cements might produce a texture similar to Figure 9C. In general, the final texture is poorly controlled by the original geometry.

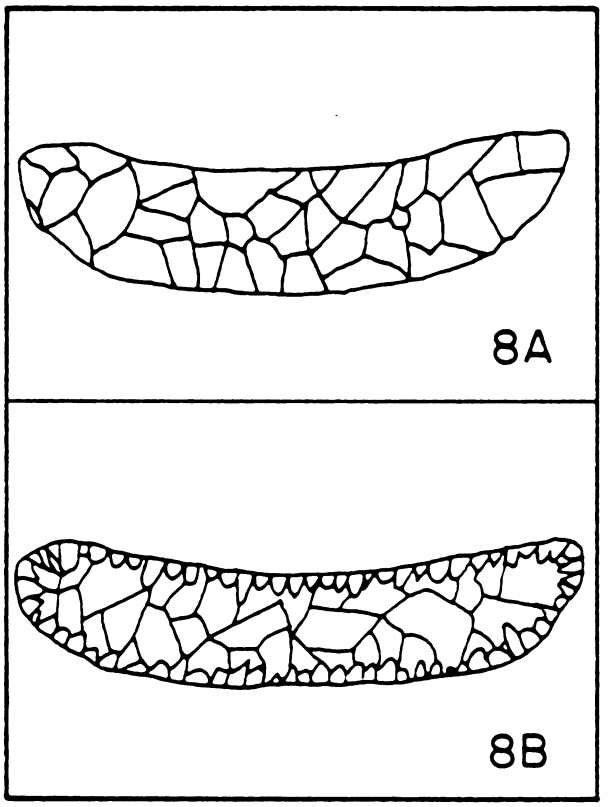
8A
8B

with respect to calcite, partially dissolve aragonitic material. The immobile water in the chalk zone then becomes supersaturated with respect to calcite and simultaneous dissolution of aragonite and precipitation of calcite occurs (Pingitore, 1976). This mechanism is generally restricted to the phreatic environment because communication between the water in the reaction zone and that of the bulk aquifer is neccessary to transport ions away from the reaction site in order to produce the moderately porous zone (Pingitore, 1976). This is analogous to the experiments of Metzger and Barnard (1968), where a smaller b term resulted in a slower transformation rate than for the powder experiments and chalky blocks were produced. Transformation through a chalk zone has been observed in studies of scleractinian coral diagenesis (James, 1974; Pingitore, 1976). The resulting neospar is relatively coarse grained with moderate retention of precursor fabric defined by inclusions (Pingitore, 1976) (Fig. 9A). Saller (1982) has observed variations in chalk zone replacement of skeletal material. Intermediate stages of marine cement diagenesis have not been observed in the rock record so that the mechanism responsible for a particular fabric only can be inferred. By analogy to the fabrics observed in skeletal material, characterized by coarse grain size and moderate loss of textural detail, coarse calcite neospar (Grover, 1981)(Fig. 9B, Table 4), may have resulted from the diagenesis of acicular marine cements by a similar mechanism. This neospar is recognized by its coarse grain size, the presence of subcrystals, undulatory extinction, and irregular crystal boundaries

Figure 9. Mesoscale dissolution-precipitation textures (chalk zone). (A) Scleractinian corals (fine crystallites, generally open secondary pore system) alter to coarse calcite neospar with moderate retention of precursor fabric (adapted from James, 1974; Pingitore, 1976). (B) Acicular marine cements (highly variable initial textures) becomes coarse calcite neospar with moderate retention of precursor fabric (adapted from Grover, 1981). (C) Radial aragonite rays transform to equant calcite with poor to moderate retention of the precursor fabric (adapted from Assereto and Folk, 1976). In general, mesoscale dissolutin-precipitation textures show moderate retention of precursor fabrics.

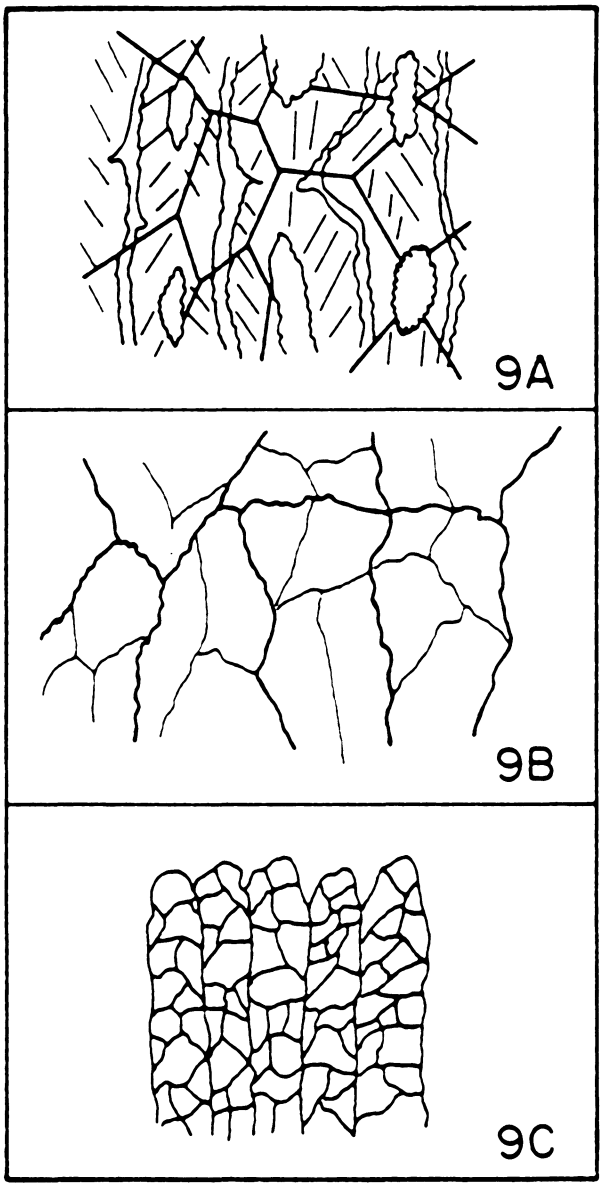
9A
9B
9C

(Grover, 1981). Based on the principle that small crystals are more soluble than larger ones, so that larger ones grow at the expense of smaller ones (Oswald ripening) this coarse neospar texture also could be the result of recrystallization of pseudoacicular calcite during burial diagenesis. This recrystallization would result in further loss precursor fabric detail often preseved in pseudoascicular neospar. An equant calcite mosaic after acicular aragonite (Assereto and Folk, 1976) (Fig. 9C) may result if the aragonite needles are loosely packed such that the original material exerts little control on the migration of fluids through the material and calcite nucleates simultaneously throughout the reaction zone. Since the general morphology of the aragonite rays is preserved (outlined by inclusions) it is doubtful that a void stage developed. The overall loss of detailed microfabric indicates transformation through a chalk zone rather than through a thin fluid film.

Microscale dissolution-precipitation through a thin fluid film from a micron (Pingitore, 1976) to less than one hundredth of a micron (Wardlaw et al. 1976) wide has the smallest effective surface area per mole of solid available to react with solution (smallest b term), and therefore, the slowest rate of transformation. Because of this very slow reaction rate, it is doubtful whether this process could be duplicated in the laboratory. It may occur either in the vadose environment, where intermittant liquid communication between the reaction zone and the bulk aquifer inhibits the development of a chalk zone (Pingitore, 1976), or in the phreatic environment where micro-

environmental variations in degree of saturation and geometry of materials may dictate transformation by one or all three of the mechanisms. Transformation through a thin fluid film in the phreatic environment, is most likely to develop the higher the degree of saturation and/or the more tightly packed the material. This type of transformation has been observed in studies of molluscan and scleractinian coral diagenesis (James, 1974; Pingitore, 1976; Wardlaw et al., 1976; Sherer, 1975). The resulting neospar may be fine (Pingitore, 1976) or coarse (Wardlaw, 1976) grained with relatively good preservation of precursor fabric.

These studies also demonstrate control of the transformation by precursor geometry on this this film process. In corals, the transformation begins in the trabecula or between loosely packed aragonite crystallites. These are the most porous regions of the skeleton, where the greater relative surface area available to react with solution makes the transformation rate greatest. The transformation then preferentially continues along intercrystalline boundaries (James, 1974; Pingitore, 1976; Sherer, 1975). Similar control of the transformation by shell ultrastructure has been observed in the study of molluscan diagenesis (Hudson, 1962; Bathurst, 1964; Hudson, 1965; Land, 1967; Schroeder, 1973). The neospar is generally anhedral with irregular crystal boundaries (Fig. 10D). Calcite crystals are often defined by organic laminae indicating control of the crystal growth by precursor fabric (Land, 1967; Schroeder, 1973). In both experimental mosaics (Land, 1967; Pingitore, 1976) and

Figure 10. Microscale dissolution-precipitation (thin film or messenger film). (A) Acicular marine cements (coarse crystallites and open secondary pore system) transform to polycrystalline divergent radial pseudospar (Mazzullo, 1980) or pseudoacicular neospar (Grover, 1981). Epitaxial nucleation occurs throughout the matrix to produce a mosaic of optically aligned calcite crystals. Acicular marine cements with coarse crystallites and a tight secondary pore system become (B) monocrystalline radiaxial fibrous calcite (Kendall and Tucker, 1973; Bathurst, 1975; Marshall, 1981) when nucleation takes place between aragonite bundles or (C) monocrystalline fascicular optic calcite (Kendall, 1977; Marshall, 1981) when nucleation occurs within each bundle. (D) Fossils (gastropods)(fine crystallites relatively open secondary pore system) become anhedral, fine to coarse grained neospar (Schroeder, 1973; Land, 1970; Wardlaw et al., 1978). The neospar shows poor to excellent retention of precursor fabrics depending upon their original geometry.

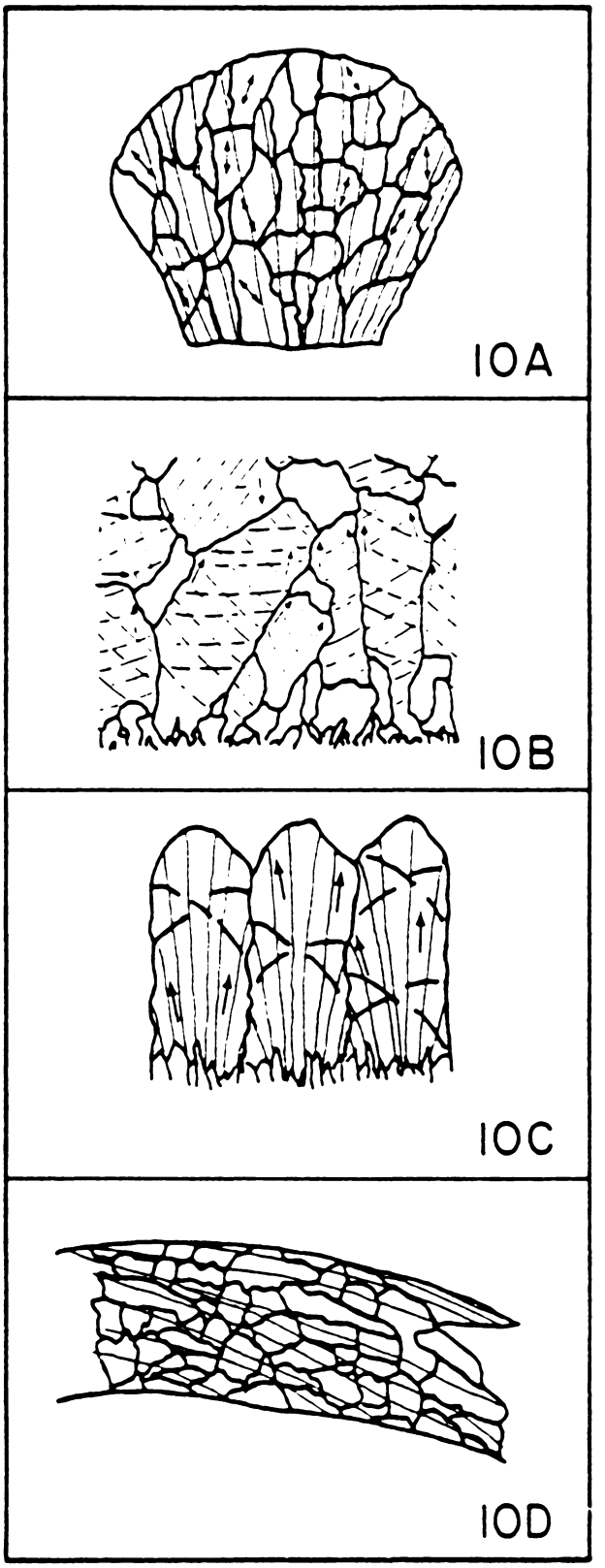
10A
10B
10C
10D

those found in the rock record, calcite is often found to nucleate epitaxially on the original aragonite such that the c-axis orientation may be preserved (Land, 1970). Also, since the transformation and growth of the calcite is most rapid along intercrystalline boundaries the original direction of crystal elongation may be preserved.

This control of transformation by the original material has also been recognized in the diagenesis of acicular marine cements (Kendall and Tucker, 1973; Marshall, 1981; Mazzollo and Cys, 1979; Mazzullo, 1980; Grover, 1981). It is proposed here that the variation in diagenetic calcite fabrics after acicular marine cements is due primarily to the differences in the original fluid/solid geometries. In samples where the aragonite acicular bundle is more loosely packed, simultaneous nucleation of calcite may occur throughout the material producing a polycrystalline mosaic. When calcite nucleates epitaxially on the original material, and the aragonite crystallographic orientation is preserved, divergent radial pseudospar (Mazzullo and Cys, 1977, 1979; Mazzullo, 1980) and/or pseudoacicular neospar (Grover, 1981) (Fig. 10A) fabrics may develop. Again, these fabrics may be subsequently recrystallized during burial diagenesis to produce coarse calcite neospar (Grover, 1981).

When bundles of acicular aragonite are so tightly packed that there is no substantial difference in intercrystalline and intracrystalline transformation rates a thin film transformation front may develop (Kendall and Tucker, 1973). This is believed to be responsible for the development of radiaxial fibrous (Kendall and

Tucker, 1973; Bathurst, 1975; Chafetz, 1979; Marshall, 1981) (Fig. 10B) and radial fibrous (fascicular optic) (Kendall, 1977; Chafetz, 1979; Marshall, 1981) (Fig. 10C) diagenetic fabrics after acicular marine cements. These neomorphic fabrics are typically coarse grained, one calcite crystal replacing a single bundle or adjacent bundles of acicular cement, with good preservation of precursor fabric (Kendall and Tucker, 1973; Marshall, 1981). The difference between radiaxial fibrous and radial fibrous (fascicular optic) calcite textures is thus controlled by whether calcite nucleates within or between bundles as proposed by Marshall, (1981).

CHAPTER IV

SUMMARY

The rate of the aqueous aragonite to calcite transformation is not only dependent on temperature (Bischoff, 1969; this study) and solution chemistry (Fyfe and Bischoff, 1965; Taft, 1967; Bischoff and Fyfe, 1968; Berner, 1975) but also on the effective surface area per mole of reactant and product available to interact with the solution. The rate equation (equation 7) verified in this study, adequately describes this dissolution-precipitation reaction and includes a geometric factor which can be modified to explain variation in rates due to variation in the surface area/solution ratios. The control of reaction rate by the relative surface area of solid available to react with the solution can be further demonstrated by comparing results of experiments run with fine discrete particles (this study; Taft, 1967) and those run with larger dense blocks (Metzger and Barnard, 1968). From Arrhenius plots (Fig. 6) of data collected from these experiments it can be shown that although the fundamental transformation mechanism is the same, i.e. dissolution-precipitation, the absolute rates differ because of geometry. The rate is much slower for the large dense blocks, in which transformation proceeds via a chalk zone (smaller effective surface area/solution ratio), than for the fine discrete particles which undergo passive dissolution-precipitation (larger effective surface area/solution ratio).

The fabric of neomorphic calcite is also dependent on the

effective surface area available to solution, i.e. the original geometry of the precursor material. The three principle transformation regimes operative during carbonate diagenesis: macroscale (passive) dissolution-precipitation, mesoscale (chalk zone) dissolution-precipitation, and microscale (thin fluid film) dissolution-precipitation are differentiated by the surface area/solution ratio in the reaction zone and must therefore influence the fabric of neomorphic calcite. One or all three of the mechanisms may develop in a single diagenetic environment depending on variations in microenvironmental conditions, i.e. solution chemisty (degree of saturation), and most importantly, the availability of solution to the reaction zone. In general the smaller the surface area/solution ratio in the reaction zone the slower the transformation rate and the higher the degree of rentention of precursor fabric in the neomorphic calcite.

BIBLIOGRAPHY

ASSERETO, R., AND FOLK, R.L., 1976, Brick-like textures and radial rays in Triassic pisolites of Lombardy Italy: a clue to distinguish ancient aragonite pisolites: Sed. Geology, v. 16, p. 205-222.

BANNER, F.T., AND WOODS, G.V., 1964, Recrystallization in microfossiliferous limestones: Geological Jour., v. 4, p. 21-34.

BATHURST, R.G.C., 1964, The replacement of aragonite by calcite in the molluscan shell wall, in Imbrie, J., and Newell, N.D., eds., Approaches to Paleoecology: New York, Wiley, p. 357-376.

_____, 1975, Carbonate sediments and their diagenesis: Developments in Sedimentology 12, Amsterdam, Elsevier, 658 p.

BERNER, R.A., 1975, The role of magnesium in the crystal growth of calcite and aragonite from seawater: Geochim. Cosmochim. Acta, v. 39, p. 489-504.

_____, AND MORSE, J.W., 1974, Dissolution kinetics of calcium carbonate in seawater IV: theory of calcite dissolution: Am. Jour. Sci., v. 274, p. 108-134.

BISCHOFF, J.L., 1969, Temperature controls on aragonite-calcite transformation in an aqueous solution: Am. Mineralogist, v. 54, p. 149-155.

_____, AND FYFE, W.S., 1968, Catalysis, inhibition and the calcite-aragonite problem, 1: the aragonite-calcite transformation: Am. Jour. Sci., v. 266, p. 65-79.

BRAND, V. AND VEIZER, J., 1980, Chemical diagenesis of a

multicomponent carbonate system-1: trace elements: Jour. Sed. Petrology, v. 59, p. 1219-1236.

BROWN, W.H., FYFE, W.S., AND TURNER, F.J., 1962, Aragonite in California glaucophane schists, and the kinetics of the aragonite-calcite transformation: Jour. Petrology, v. 3, p. 566-582.

CARLSON, W.D., AND ROSENFIELD, J.L., 1981, Optical determination of topotactic aragonite-calcite growth kinetics: metamorphic implications: Jour. Geol., v. 89, p. 615-638.

CHAFETZ, H.S., 1979, Petrology of carbonate nodules from a Cambrian tidal inlet accumulation, central Texas: Jour. Sed. Petrology, v. 49, p. 215-222.

CHAUDRON, G., 1954, Contribution a l'etude des reactions dans l'etat solide cinetique de la transformation aragonite-calcite, in Hemlin, E., ed., Proc. Intern. Symp. Reactivity Solids, Gothenburg, 1952: Ingeniorsvetenskapsakademien och Chalmers Tekniska Hogskola, Goteborg, p. 9-20.

COTTER, E., 1966, Limestone diagenesis and dolomitization in Mississippian carbonate banks in Montana: Jour. Sed. Petrology, v. 36, p. 764-774.

DAVIES, G.R., 1976, Early marine and later postburial cementation and diagenesis of Paleozoic carbonate rocks, Artic Archipelago: Am. Assoc. Petroleum Geologists Bull., v. 60, p. 662-663.

_____, 1977, Former magnesium calcite and aragonite submarine cements in upper Paleozoic reefs of the Canadian Artic: a summary: Geology, v. 5, p. 11-15.

DAVIES, B.L., AND ADAMS, L.H., 1965, Kinetics of calcite aragonite transformation: Jour. Geophs. Res., v. 70, p. 433-441.

DAVIES, T., AND HOOPER, P., 1963, The determination of the calcite:aragonite ratio in mollusc shells by X-ray diffraction: Mineral Mag., v. 33, p. 608.

DODD, J.R., 1966, Processes of conversion of aragonite to calcite with examples from the Cretaceous of Texas: Jour. Sed. Petrology, v. 36, p. 733-741.

DUNHAM, R.J., 1971, Meniscus cement, in Bricker, O.P., ed., Carbonate Cements: Baltimore, Johns Hopkins, p. 297-300.

FOLK, R.L., 1973, Carbonate petrography in the post-Sorbian age, in Ginsburg, R.N., ed., Evolving Concepts in Sedimentology: Johns Hopkins Univ., Studies in Geology, No. 21, p. 118-158.

_____, 1974, The natural history of crystalline calcium carbonate: effect of magnesium content and salinity: Jour. Sed. Petrology, v. 44, p. 40-53.

FRIEDMAN, G.M., 1975, Address of the retiring president Soc. Econ. Paleontologists Mineralogists: The making and unmaking of limestones or the ups and downs of porosity: Jour. Sed. Petrology, v. 45, p. 379-398.

FYFE, W.S., AND BISCHOFF, J.L., 1965, The calcite-aragonite problem: Soc. Econ. Paleontologists Mineralogists Spec. Paper No. 13, p. 3-13.

GROVER, G.A., 1981, Cement types and cementation patterns of Middle Ordovician ramp-to-basin carbonates, Virginia [unpub. PhD.

thesis]: Blacksburg, V.P.I. and S.U., 220 p.

HALLAM, A., AND O'HARA, M.J., 1962, Aragonite fossils in the Lower Carboniferous of Scotland: Nature, v. 195, p. 273-274.

HUDSON, J.D., 1962, Pseudo-pleochroic calcite in recrystallized shell limestones : Geol. Mag., v. 99, p. 492-500.

_____, 1965, Preservation and recrystallization in some Jurassic molluscan shells from Scotland (abs.): Geol. Soc. Am. Spec. Paper No. 82, p. 98.

JAMES, N.P., 1974, Diagenesis of scleractinian corals in the subaerial vadose environment: Jour. Paleontology, v. 48, p. 785-799.

KATZ, A., 1973, The interaction of magnesium with calcite during crystal growth at 25°C-90°C and 1 atm.: Geochim. Cosmochim. Acta, v. 37, p. 1563-1586.

KENDALL, A.C., 1971, Internal sediment as a criterion of void filling cement, in Bricker, O.P., ed., Carbonate Cements: Baltimore, Johns Hopkins, p. 303-307.

_____, 1977, Fascicular-optic calcite: a replacement of bundled acicular carbonate cements: Jour. Sed. Petrology, v. 47, p. 1056-1062.

_____, AND TUCKER, M.E., 1973, Radiaxial fibrous calcite: a replacement after acicular carbonate: Sedimentology, v. 20, p. 365-389.

KINSMAN, D.J.J., 1969, Interpretation of Sr^{2+} concentrations in carbonate minerals and rocks: Jour. Sed. Petrology, v. 39, p. 486-508.

KUNZLER, R.H., AND GOODELL, H.G., 1970, The aragonite-calcite transformation: a problem in kinetics of a solid-state reaction: Am. Jour. Sci., v. 269, p. 360-391.

LAND, L.S., 1967, Diagenesis of skeletal carbonates: Jour. Sed. Petrology, v. 37, p. 914-930.

_____, 1970, Phreatic versus vadose meteoric diagenesis of limestones: Evidence from a fossil water table: Sedimentology, v. 14, p. 175-185.

LASAGA, A.C., 1981, Rate laws of chemical reactions, in Lasaga, A.C., and Kirkpatrick, R.J., eds., Reviews in Mineralogy, Kinetics of Geochemical Processes, v. 8, p. 1-68.

LOHMANN, K.C., 1978, Closed system diagenesis of high magnesium calcite and aragonite cement: Joint Ann. Mtg. Geol. Soc. Am., Geol. Assoc. Canada, Min. Assoc. Canada, Abstracts with Programs, v. 3, p. 446.

LONGMAN, M.W., 1980, Carbonate diagenetic textures from near surface diagenetic environments: Am. Assoc. Petroleum Geologists Bull., v. 64, p.

MARSHALL, J.D., 1981, Zoned calcite in Jurassic ammonite chambers: trace element, isotopes, and neomorphic origin: Sedimentology, v. 28, p. 867-887.

MATTHEWS, R.K., 1968, Carbonate diagenesis: Equilibration of sedimentary mineralogy to the subaerial environment: coral cap of Barbados, W.I.: Jour. Sed. Petrology, v. 38, p. 1110-1119.

_____, 1974, A process approach to diagenesis of reefs and reef

associated limestones, in Laporte, L.F., ed., Reefs in Time and Space: Soc. Econ. Paleontologists Mineralogists Spec. Pub. 18, p. 234-256.

MAZZULLO, S.J., 1980, Calcite pseudospar replacive of marine acicular aragonite and implications for aragonite cement diagenesis: Jour. Sed. Petrology, v. 50, p. 409-422.

_____, AND CYS, J.M., 1977, Submarine cements in Permian boundstones and reef associated rocks, Guadalupe Mountains, West Texas and Southeastern New Mexico, in Hileman, M.E. and Mazzullo, S.J., eds., Upper Guadalupe Mountains New Mexico and West Texas: Soc. Econ. Paleontologists Mineralogists Publication 77-16, p. 151-200.

_____, AND _____, 1979, Marine aragonite seafloor growths and cements in Permian phylloid algal mounds Sacramento Mountains New Mexico: Jour. Sed. Petrology, v. 49, p. 917-936.

METZSGER, Wm.J., AND BARNARD, W., 1968, Transformation of aragonite to calcite under hydrothermal conditions: Am. Mineralogist, v. 53, p. 295-301.

MULLER, G., 1971, Gravitational cement: an indicator for the vadose zone of the subaerial diagenetic environment, in Bricker, O.P., ed., Carbonate Cements: Baltimore, Johns Hopkins, p. 301-302.

PINGITORE, N.E., 1976, Vadose and phreatic diagenesis: processes, products and their recognition in corals: Jour. Sed. Petrology, v. 46, p. 985-1006.

_____, 1982, The role of diffusion during carbonate diagenesis: Jour. Sed. Petrology, v. 52, p. 27-39.

PLUMMER, L.N., PARKHURST, D.L., AND WIGLEY, T.M.L., 1979, Critical review of the kinetics of calcite dissolution and precipitation, in Jenne, E.A., ed., Chemical Modeling in Aqueous Systems: A.C.S. Symposium Series 93, p. 537-573.

RAO, M.S., 1973, Kinetics and mechanisms of transformation of aragonite calcite: Indian Jour. Chem., v. 11, p. 280-283.

SALLER, A. H., 1982, Patterns of dissolution and neomorphism in Pleistocene limestones of Enewetak atoll: Geo. Soc. America, Abstracts with Programs, v. 14, p. 607.

SANDBERG, P.A., 1981, Aragonite diagenesis and strontium content of limestones: interrelationships and temporal trends: Geo. Soc. America, Abstracts with Programs, v. 13, p. 545.

SCHMALZ, R.F., 1967, Kinetics and diagenesis of carbonate sediments: Jour. Sed. Petrology, v. 43, p. 1012-1020.

SCHROEDER, J.H., 1973, Submarine and vadose cements in Pleistocene Bermuda reef rock: Sed. Geology, v. 10, p. 179-204.

SHERER, M., 1975, Cementation and replacement of Pleistocene corals from the Bahamas and Florida: diagenetic influence of non marine environments: N. Jb. Geol. Palaont. Abh., v. 149, p. 259-285.

SJOBERG, E.L., 1976, A fundamental equation for calcite dissolution kinetics: Geochim. Cosmochim. Acta, v. 40, p. 441-447.

STEINEN, R.P., AND MATTHEWS, R.K., 1973, Phreatic versus vadose diagenesis: stratigraphy and mineralogy of a cored bore hole on Barbados, West Indies: Jour. Sed. Petrology, v. 43, p. 1012-1020.

SUESS, E., 1970, Interaction of organic compounds with calcium

carbonate -I: Association phenomena and geochemical implications: Geochim. Cosmochim. Acta, v. 34, p. 157-168.

TAFT, W.H., 1967, Physical chemistry of formation of carbonates, in Chilingar, G.V., Bissell, H.J. and Fairbridge, R.W., eds., Carbonate Rocks V. 2: New York, Elsevier, p. 151-168.

TURNBULL, D., 1956, Phase changes: Solid State Phys., v. 3, p. 225-306.

WALTER, L.M., AND HANOR, J.S., 1979, Orthophosphate: effect on the relative stability of aragonite and magnesium calcite during early diagenesis: Jour. Sed. Petrology, v. 49, p. 937-944.

WARDLAW, N., OLDERSHAW, A., AND STOUT, M., 1978, Transformation of aragonite to calcite in a marine gastropod: Canadian Jour. Earth Sci., v. 15, p. 1861-1866.

WINLAND, H.D., 1969, Stability of calcium carbonate polymorphs in warm, shallow seawater: Jour. Sed. Petrology, v. 39, p. 1579-1587.

APPENDIX 1

EXPERIMENTAL METHODS

Synthesis of Materials

Synthetic aragonite was prepared following the proceedure of Katz (1973). The solutions, 0.05m $NH_4(CO_3)_2$and $CaCl_2$, were prepared from Baker chemical reagents. One liter of each solution was heated to 80°C. The $CaCl_2$ solution was then added at a rate of 285 ml/min to the $NH_4(CO_3)_2$ solution while stirring rapidly. This produced approximately 3 grams of 97-99% pure aragonite (the balance was calcite). When 100% aragonite was required $MgCl_2$ was added to the $CaCl_2$ solution to produce 0.02 m Mg^{2+} prior to heating. The precipitate was rinsed five times with distilled water, then with acetone and air dried. The proceedure was repeated nine times in order to collect approximately 25 grams of material. The actual run material consisted of 95% aragonite needles (averaging 13.6 µm long X 2.75 µm diameter and ranging from 30 µm X 5 µm to 5 µm X 2 µm) 5% calcite rhombs (averaging 5.3 µm on an edge and ranging from 13 µm to 2 µm on an edge). The calcite was produced by transforming the synthetic aragonite in 6 ml of distilled deionized water at 101±1.0°C (see later). Complete transformation was achieved after 15 hours. The calcite was mixed with aragonite as an acetone slurry with mortar and pestle. It was then dried, sieved through a fine silk screen, and X-rayed five times

to determine the homogeneity of the mixture. The 95% aragonite mixture was chosen for this study in order to minimize the nucleation effects.

Transformation Runs

1) 0.200±0.0005g of the 95% aragonite, 5% calcite, run material were placed in 10 ml Teflon bombs and then preheated at the appropriate run temperature for 45-60 minutes.

2) 6 ml of distilled deionized water preheated to the run temperature was then added to each sample. At this point timing for the reaction began.

3) The bombs were maintained at the run temperature for appropriate intervals and then immediately quenched in a cold water bath. The supernatent water was then removed from the bomb and the run solids were transferred to a glass vial and dried.

4) The samples were then X-rayed (see later) and percent calcite determined.

The experiment was run at three temperatures: 101±1.0°C and 77±1.0°C in a Fisher Econtemp Laboratory Oven and 50±0.5°C in a Tecam Constant Temperature Bath. Ten to fifteen samples were necessary to define each rate curve.

X-Ray Diffraction

A Norelco automated X-ray diffractometer with nickel-filtered, CuKα radiation (20 ma and 40 KV) was used to characterize the run material. Each sample was both step scanned and continuously scanned from 25° to 30° in 2θ. The intensities of the aragonite {111} and {012} reflections and the calcite {1012} reflection were measured. The percent calcite in the run products was determined using a correlation chart constructed according to Davies and Hooper (1965) (Fig. 11, Table 5), in which $(I_{C1012}/I_{A111}+I_{A012}+I_{C1012})$ X 100 was plotted versus the weight percent calcite in the mixture. Each sample was mounted on a glass slide using Scotch brand double stick tape. The run product was sieved onto the slide through a fine mesh silk screen sieve and then flattened with a glass slide. This minimized the effect of calcite preferred orientation. Each sample was X-rayed approximately four times. Successive X-ray measurements of one sample were within 3% of each other in 80% of the samples, 5% of each other in 85%, and 8% of each other in 100%.

Figure 11. Correlation Chart: $(I_{C1012}/I_{A111}+I_{A012}+I_{C1012})$ X 100 versus mole fraction calcite, constructed after Davies and Hooper (1965).

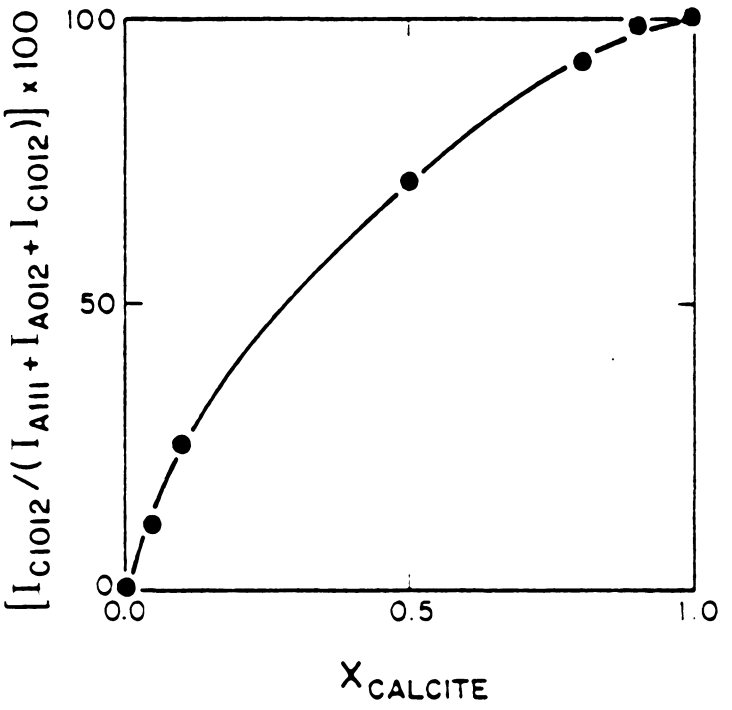
100
50
0
0.0
0.5
1.0
$[I_{C1012}/(I_{A111}+I_{A012}+I_{C1012})] \times 100$
$X_{CALCITE}$

TABLE 5. Correlation chart data

X	$(I_{C1012}/I_{A111}+I_{A012}+I_{C1012})X100$
1.00	100.0
0.90	98.5
0.80	92.3
0.50	71.5
0.10	25.5
0.05	11.4

The vita has been removed from the scanned document

THE AQUEOUS ARAGONITE TO CALCITE TRANSFORMATION: RATE, MECHANISMS, AND ITS ROLE IN THE DEVELOPMENT OF NEOMORPHIC FABRICS

by

Kathleen Mary McManus

(ABSTRACT)

The rate of the aqueous transformation of aragonite to calcite was measured at 50°, 77°, and 101°C. The observed mole fraction calcite versus time relationship can be fit by the integrated rate model:

$$t = [(3/C_2)(1-X)^{2/3} + (3/C_1)(X^{2/3})]/[K_2-K_1]$$

The constants C_1 and C_2 combine geometric factors, especially relative surface areas of the solids, K_1 and K_2 are the thermodynamic equilibrium constants for aragonite and calcite respectively. Apparent activation energies (E_A') and absolute rates were calculated from Arrhenius plots of data from this study and others:

	E_A'	Conditions	Material	Time-50% CAL 25°C
Metzger and Barnard, 1968	58 kJ mol^{-1}	wet	cm cubes	$2.25X10^{2}$yr
Taft, 1967	67	wet	syn. powder	$2.0X10^{-1}$
This study	55	wet	syn. powder	$5.7X10^{-2}$
Brown et al., 1962	373	dry		$4.7X10^{33}$

The E_A for this study is comparable with that of Metzger and Barnard indicating a similar mechanism, but absolute rates differ dramatically because of the different geometries of the run material. The dry transformation rates are so slow at diagenetic temperatures that this mechanism is of no importance geologically.

Because the rate of the transformation is dependent on the geometry of the reacting system it is not surprising that most studies of neomorphic calcites find that the calcite textures are related to the original aragonite textures. Three transformation regimes, macroscale (passive dissolution), mesoscale (chalk zone), and microscale (thin film) dissolution-precipitation, are proposed to explain the variability in observed diagenetic calcite textures. These are differentiated by the surface area/solution ratio in the reaction zone. In general the smaller the geometric factor in the rate equation, i.e. the smaller the surface area/solution ratio, the slower the transformation rate and the higher the degree of precursor fabric retention in the neomorphic calcite.